

UCLA

UCLA Previously Published Works

Title

Global changes in diffusion tensor imaging during acute ischemic stroke and post-stroke cognitive performance.

Permalink

<https://escholarship.org/uc/item/2wx8105g>

Journal

Cerebrovascular and brain metabolism reviews, 42(10)

Authors

Kern, Kyle

Wright, Clinton

Leigh, Richard

Publication Date

2022-10-01

DOI

10.1177/0271678X221101644

Peer reviewed

Global changes in diffusion tensor imaging during acute ischemic stroke and post-stroke cognitive performance

Kyle C Kern¹ , Clinton B Wright¹ and Richard Leigh^{1,2} 

Abstract

Post-stroke cognitive impairment is related to the effects of the acute stroke and pre-stroke brain health. We tested whether diffusion tensor imaging (DTI) can detect acute, global effects of stroke and predict post-stroke cognitive performance. Patients with stroke or TIA enrolled in a prospective cohort study were included if they had 1) at least one DTI acquisition at acute presentation, 24 hours, 5 days, or 30 days, and 2) follow-up testing with the telephone Montreal Cognitive Assessment (T-MoCA) at 30 and/or 90 days. A whole brain, white-matter skeleton excluding the infarct was used to derive mean global DTI measures for mean diffusivity (MD), fractional anisotropy (FA), free water (FW), FW-corrected MD (MD_{tissue}), and FW-corrected FA (FA_{tissue}). In 74 patients with ischemic stroke or TIA, there was a transient 4.2% increase in mean global FW between acute presentation and 24 hours ($p = 0.024$) that returned to initial values by 30 days ($p = 0.03$). Each acute global DTI measure was associated with 30-day T-MoCA score ($n = 61$, $p = 0.0011$ – 0.0076). Acute global FW, MD, FA and FA_{tissue} were also associated with 90-day T-MoCA ($n = 56$, $p = 0.0034$ – 0.049). Transient global FW elevation likely reflects stroke-related interstitial edema, whereas other global DTI measures are more representative of pre-stroke brain health.

Keywords

Acute ischemic stroke, diffusion tensor imaging, free water, magnetic resonance imaging, post-stroke cognitive impairment, vascular cognitive impairment

Received 28 October 2021; Revised 28 March 2022; Accepted 18 April 2022

Introduction

Cognitive impairment is common after stroke,¹ and stroke more than doubles the lifetime risk of dementia.^{2,3} Stroke severity and/or strategic infarct location are important predictors of cognitive dysfunction after stroke. However, baseline clinical demographics, recurrent stroke, and the pre-stroke burden of subclinical cerebrovascular disease also increase risk for post-stroke cognitive impairment.⁴ While it is known that incident stroke is associated with cognitive decline⁵ independent of stroke location,⁶ the mechanism of post-stroke cognitive impairment and dementia is not known.

Prior studies have demonstrated that the severity of leukoaraiosis, a late marker of subclinical cerebrovascular disease burden, is associated with worse functional outcomes and increased risk for post-stroke dementia.^{7,8} The integrity of distributed brain networks

contributes to baseline cognitive performance,⁹ and disruption of these networks due to stroke is associated with cognitive impairment^{10,11} and impaired recovery.^{12,13} For this reason, markers of global brain health are complementary to measures of stroke severity in predicting cognitive outcome. But stroke also causes acute global brain changes^{14,15} and a systemic inflammatory response¹⁶ that is also related to stroke outcome.^{17,18} Global brain measures that are

¹National Institute of Neurological Disorders and Stroke, National Institutes of Health, Bethesda, MD, USA

²Department of Neurology, Johns Hopkins University School of Medicine, Baltimore, MD, USA

Corresponding author:

Richard Leigh, 600 N. Wolfe Street, Phipps 4, Suite 446, Baltimore, MD 21287, USA.

Email: rleigh4@jhu.edu

sensitive to acute stroke-related effects such as neuroinflammation may be prognostic of post-stroke cognitive impairment. One such measure of global brain health is white matter microstructural integrity, which can be measured using diffusion tensor imaging (DTI).

DTI measures the directional diffusivity of water, thereby revealing breakdown of tissue microarchitecture or fluid shifts between the intracellular, extracellular, or vascular spaces.^{19,20} Conventional DTI metrics, including mean diffusivity (MD) and fractional anisotropy (FA), are altered in chronic cerebrovascular disease even in normal appearing white matter²¹ and are associated with cognitive performance.²² Chronic white matter injury manifests as increased MD and decreased FA. However, these conventional DTI metrics can be further refined by isolating the effects of extracellular free water (FW).

FW fraction can be extracted from DTI using a 2-compartment model of the diffusion signal in brain tissue: a freely diffusing (isotropic) compartment with the diffusivity of water and a directional, tissue tensor compartment.^{23,24} DTI models that include additional model constraints permit FW estimation using typical clinical DTI acquisitions.^{24,25} FW can be seen as a contaminant of MD and FA for which these metrics need to be corrected. However, FW itself has pathologic implications. FW is a sensitive marker of chronic cerebrovascular disease^{26,27} that is closely associated with vascular cognitive impairment^{28,29} and systemic markers of inflammation.³⁰ FW is implicated as an indirect marker of subtle neuroinflammation in other brain pathologies including Alzheimer's disease,³¹ depression,³² and schizophrenia.³³ The effects of acute ischemic stroke on local or global free water measures are unknown.

Prior studies of ischemic stroke patients have demonstrated that DTI measurements remote from the infarct in the late acute to subacute stage are associated with post-stroke cognitive impairment.^{34,35} However, ischemic stroke leads to global brain changes acutely¹⁵ that may also contribute to post-stroke cognitive performance but may not be captured in later time periods. We hypothesized that global DTI measures at the time of acute stroke would reflect not only underlying brain health due to chronic cerebrovascular changes, but also diffuse, dynamic changes in response to focal ischemia. Specifically, we hypothesized that global changes in DTI measures in the acute post-stroke period, in particular global FW, would be sensitive to fluid shifts remote from the focal ischemia and may reflect a stroke-related inflammatory response. For the current study, we measured DTI, including FW, at the time of acute stroke presentation and longitudinally thereafter to compare global DTI measures with post-stroke cognitive performance.

Methods

Standard protocol approvals, registrations, and patient consents

The study protocol was approved by the National Institutes of Health (NIH) Institutional Review Board (approval number 01N0007), which determines ethical guidelines for NIH clinical research that are in accordance with the Council for International Organizations of Medical Sciences International Ethical Guidelines for Health-related Research Involving Humans. All patients signed written informed consent.

Study population

The study population included subjects enrolled in the NIH Natural History of Stroke Study (clinicaltrials.gov: NCT00009243), an observational cohort study of acute ischemic stroke patients. Participants were recruited from two regional stroke centers affiliated with the NIH Intramural Stroke program: Medstar Washington Hospital, Washington DC and Suburban Hospital, Bethesda, MD.

Patients presenting between October 2018 and February 2020 were recruited if they had a diagnosis of stroke or TIA and were imaged with MRI. Stroke or TIA was diagnosed clinically by a stroke neurologist if the patient had acute onset neurologic symptoms with the aid of MRI to exclude alternative diagnoses. Patients were included in the study if they had at least one MRI with DTI during the acute hospitalization and were tested with the Montreal Cognitive Assessment (MoCA) at follow-up either in-person or by telephone at 30 and/or 90 days.³⁶ At 30-days, patients underwent either the full MoCA (in-person, score out of 30) or the telephone MoCA (T-MoCA), which is a subset of the MoCA³⁷ that is scored out of 22. At 90-days patients were tested with the T-MoCA. While we report the full MoCA score for the subset of patients with 30-day in-person testing, we also report T-MoCA for all patients tested at 30-days. Only T-MoCA scores were used in regression analyses. MRIs were included in the analysis if they were performed at the following approximate timepoints: at acute presentation, 24 hours after onset, 5 days after onset, or 30 days after onset.

MRI protocol

Brain MRIs were acquired on a 3 T Skyra scanner with a 20-channel head and neck coil and software syngo MR E11 (Siemens, Erlangen, Germany) at Suburban Hospital or a 3 T Acheiva scanner with an 8-channel head coil and software MR 5.3.1.4 (Phillips, Best, the

Netherlands) at MedStar Washington Hospital. Whole-brain DTI for the Skyra included diffusion weighted echo planar images acquired in 12 noncollinear directions at a b-value of 1000 s/mm^2 and 4 non-directional images with a b-value of 0 s/mm^2 . DTI scan parameters are repetition time (TR) = 7800 ms, echo time (TE) = 81 ms, field of view (FOV) = 220 mm, acquisition matrix = 128×128 , resolution $1.7 \times 1.7 \text{ mm}$, slice thickness = 3.5 mm, and number of excitations (NEX) = 2. Skyra FLAIR images had TR = 9000 ms, TE = 122 ms, TI = 2500 ms, flip angle = 150, FOV = 220 mm, acquisition matrix = 256×192 , resolution $0.86 \times 0.86 \text{ mm}$, slice thickness 3.5 mm. DTI for the Achieva included 15 directions at $b = 1000 \text{ s/mm}^2$ and 1 $b = 0$ image, and scan parameters TR = 4550 ms, TE = 63 ms, FOV = 240 mm, matrix = 118×118 , resolution $2 \times 2 \text{ mm}$, slice thickness = 3.5 mm, NEX = 2]. Achieva FLAIR images had TR = 9000 ms, TE = 120 ms, TI = 2600 ms, flip angle = 90, FOV = 240 mm, acquisition matrix = 240×210 , interpolated to resolution = $0.47 \times 0.47 \text{ mm}$, and slice thickness 3.5 mm.

MRI processing

DTI data was analyzed using the FMRIB Software Library v6.0 (fsl.fmrib.ox.ac.uk)³⁸ and DIPY 1.4 (dipy.org).³⁹ DTI data was corrected for eddy current distortions and motion using FSL's Eddy⁴⁰ and a tensor was fit at each voxel. A single-shell free water (FW) model was applied using DIPY.^{25,41} To generate FW maps, a two-compartment model was fit that included the tissue tensor and an isotropic FW compartment with the diffusivity of water at 37 degrees as described by Pasternak et. al.²⁴ Fitting was accomplished using a spatially regularized gradient descent algorithm. Parameters were initialized using a hybrid model that incorporates the B0 signal and the conventionally calculated MD map as described by Golub et. al.²⁵ The resulting images included conventional DTI metrics FA and MD, and novel metrics FW, FA corrected for FW (FA_{tissue}), and MD corrected for FW (MD_{tissue}). A trace image was calculated as the geometric mean of the diffusion weighted images.

The acute infarct was segmented on the scan closest to 24 hours from presentation using the trace and MD maps and a tissue classification algorithm⁴² that was trained on a separate dataset of 45 manually delineated ischemic infarcts from scans also acquired 24-hours from acute stroke presentation. The algorithm performed with a mean Dice coefficient of 0.72 in leave-one-out analysis. Segmentations were visually inspected and manually corrected for accuracy. For each patient, a rigid alignment was used to project the 24-hour infarct mask to all timepoints. This mask was dilated by 2 voxels and used to exclude infarcted

tissue from calculated global DTI measures. Masks were visually inspected at each timepoint to ensure that the entirety of the infarct and local visible diffusion changes would be excluded from the global region-of-interest (ROI). Mean DTI metrics were also derived within the non-dilated infarct mask over time and used as a comparison. Infarct location was classified as bilateral cerebrum, right cerebrum, left cerebrum, posterior fossa or none (for TIA).

Tract-based spatial statistics⁴³ was used to nonlinearly align FA maps to an atlas and create a symmetric average FA skeleton of the supratentorial white matter. The skeletonisation technique performs a local search from the atlas skeleton to select voxels with the highest FA for each individual at each timepoint. Each timepoint's skeleton was thresholded at $FA = 0.3$, and projected back into individual DTI space. In this manner, skeletonisation selects the most robust, centermost voxels of white matter bundles to minimize effects of partial voxel volumes or minor misalignment to create a region-of-interest (ROI) that is reproducible across time and subjects. The infarct mask, dilated by 2 voxels, was removed from the skeleton to create an ROI of global, non-infarcted white matter (Figure 1). Skeletons were visually inspected to ensure visible diffusion changes around the acute infarct were excluded. Mean global DTI metrics were calculated within this ROI for each subject and timepoint.

FLAIR white matter hyperintensities (WMH) were segmented on the initial scan using the lesion prediction algorithm of Lesion Segmentation Toolkit (LST)⁴⁴ and thresholded at 0.3 lesion probability. Segmentations were visually inspected and false positives in the CSF due to pulsation artifact and choroid plexus were removed. Total baseline WMH volume was calculated as a probability-weighted partial volume estimate and converted to a percentage of the total intracranial volume to correct for head size.

Statistical analysis

Statistical analysis was performed using STATA 13 (stata.com).⁴⁵ Descriptive statistics include mean and standard deviation for normally distributed variables and median and interquartile range (IQR) for non-normally distributed variables. Normality was tested with the Shapiro-Wilk test. Paired T-test was used to assess change in T-MoCA score. Distributional differences between groups were tested using a Chi-Square test. Changes in DTI measures over timepoints were estimated using mixed-effects linear regression to account for repeated measures and missing timepoints. Random effects included intercept for patients while fixed effects included timepoint, age, sex, hospital

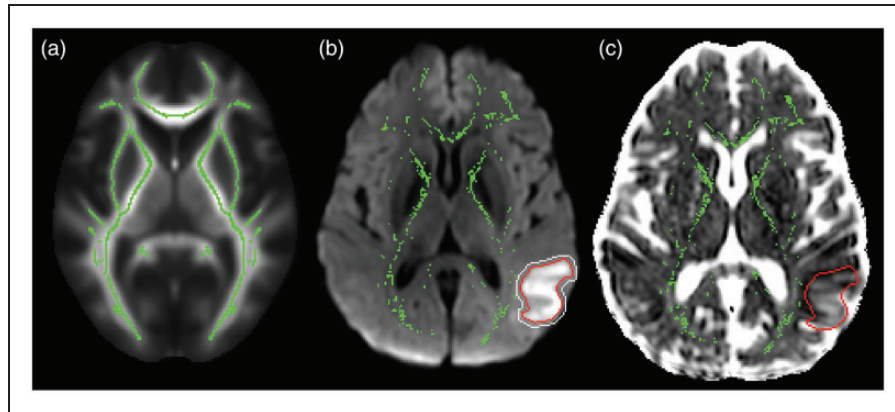


Figure 1. Global and infarct regions-of-interest (ROI) (a) A group-averaged fractional anisotropy map (background) was used to create a white matter skeleton (green) using Tract-based spatial statistics. The skeleton was projected back into patient DTI space to create an ROI. (b) A patient's trace image (background) and mean diffusivity image were used to segment the acute infarct (red outline) at the 24-hour timepoint, dilate it by 2 voxels (white outline) and exclude it from the individual white matter skeleton ROI (green) and (c) ROIs were applied to DTI metrics including free water (FW) images (background) to derive mean global FW within the skeleton ROI (green) and mean FW within the infarct ROI (red outline).

site, National Institutes of Health Stroke Scale (NIHSS), and infarct volume. Models were assessed for aptness by inspecting residual plots. Four post-hoc comparisons were adjusted using the Holm method with an alpha of 0.05. DTI measures were analyzed separately due to multicollinearity.

To identify predictors of cognitive performance at follow-up, we first performed univariate regressions between each predictor and performance on the 30-day T-MoCA (in-person or by telephone) and 90-day T-MoCA. Covariate predictors included hospital site, age, sex, pre-stroke modified Rankin score (mRS), acute NIHSS, infarct volume, education level (12 years or less vs. greater than 12 years), stroke location, and, for 30-day T-MoCA score, telephone vs. in-person administration. The overall effect of stroke location relative to the left cerebrum location was tested with a Wald test. Subsequently, multiple linear regression models included age, sex, and covariates with univariate associations with $p < 0.10$. Global white matter measures, including baseline WMH volume and acute global DTI measures, had high multicollinearity and so were tested in separate linear regression models. For each predictor, the regression coefficient, 95% confidence interval, t-statistic, p-value, adjusted R^2 for the full model, and Akaike Information Criterion (AIC) for the model are reported.

To distinguish the effects of baseline global brain health from acute stroke-related global changes on post-stroke cognitive performance, we compared the relative effects on cognitive performance of acute global FW measures and stroke-related global FW changes. To calculate stroke-related global FW changes, we imputed missing FW timepoints and

calculated the area under the FW curve (AUC) for each patient. Missing FW timepoints were imputed 30 times using multiple imputation chained equations with a regression model including FW measures, age, sex, hospital site, mRS, NIHSS, infarct volume, time from symptom discovery to MRI, 30-day T-MoCA and 90-day T-MoCA. Linear regressions were performed to test the association between FW AUC and 30 and 90 day T-MoCA, first univariate regressions (reporting t-statistic) and then multiple linear regressions including covariates selected through univariate analysis. Thirty imputed regressions were performed, and results were pooled.

Data availability

Anonymized data will be made available upon request to the corresponding author.

Results

Seventy-four patients with acute ischemic stroke or TIA were enrolled in this study, 63 had a MoCA test at 30 days either in-person (51) or by telephone (12), and 58 had a T-MoCA at 90 days. Mean age (\pm standard deviation) was 67 ± 15 years and 47% were female. While 72 of 74 patients underwent MRI at initial stroke presentation in the emergency room, 2 underwent CT first and only had DTI data from 24 hours onward. Sixty-eight patients were imaged acutely with MRI within 24 hours of symptom onset, with median time from symptom onset to imaging of 3.2 ± 5.0 hours. Four patients underwent MRI upon acute presentation to the emergency room due to acutely worsening symptoms, but initial symptom onset was

determined to be greater than 24 hours from imaging. Six patients had diffusion imaging negative TIA, two of which had a transient perfusion delay in a vascular territory consistent with symptoms. Nineteen patients received intravenous alteplase alone, 8 received endovascular therapy alone, and 6 received alteplase and endovascular therapy. Infarct locations are depicted on a group infarct overlap map (Supplemental Figure I). Demographic data and clinical measures are shown in Table 1 and Table 2.

For patients who had in-person MoCA testing at 30 days, median MoCA score was 26 ± 5 ($n=49$, score out of 30). For all patients tested with MoCA or T-MoCA at 30 days, median T-MoCA score was 18 ± 4 ($n=63$, score out of 22). Median T-MoCA score at 90 days was 19 ± 3 ($n=58$). In 47 patients with both 30 and 90-day T-MoCA, score increased by 0.7 ± 2.3 points ($p=0.03$). (Supplemental Figure II)

Temporal changes in global DTI measures

Seventy-two patients had an acute MRI timepoint, 48 had a 24-hour timepoint (range 16–39 hours), 52 had a 5-day timepoint (range 3 to 7 days), and 50 had a 30-day timepoint (range 21 to 47 days). There was a transient increase in mean global FW between the acute and 24-hour scans of 4.2% ($\text{Beta}=0.0055$,

CI: 0.0016 to 0.0094, $z=2.77$, adjusted p -value 0.023) followed by a subsequent decrease over the next two timepoints of 2.6% between the 24-hour and 30-day scans ($\text{Beta}=-0.0058$, CI: -0.010 to -0.0014 ; $z=-2.57$, adjusted $p=0.040$) (Figure 2). Main effects included higher global FW in women ($\text{Beta}=0.016$, CI: 0.0045 to 0.029, $z=2.69$, $p=0.007$) and older patients ($B=0.0013$, CI: 0.00085 to 0.0017, $z=6.30$, $p<0.001$). Global MD increased by 1.0% between the acute scan and 24 hours ($\text{Beta}=6.10 \times 10^{-6}$, CI: 1.21×10^{-6} to 1.1×10^{-5} , $z=2.45$, adjusted $p=0.058$), then decreased

Table 2. Stroke and clinical measures.

Clinical measures	
Pre-admission mRS, $n=73$; n (%)	
0	63 (86%)
1	6 (8%)
2	3 (4%)
3	1 (1%)
Admit NIHSS, $n=74$, median \pm IQR	2 \pm 4
Infarct Volume, $n=74$, median \pm IQR, cc	1 \pm 7
30-day MoCA, $n=51$, median \pm IQR	26 \pm 5
30-day T-MoCA $n=63$, median \pm IQR	18 \pm 4
90-day T-MoCA $n=58$, median \pm IQR	19 \pm 3
90-day mRS, $n=63$, n (%)	
0	22 (35%)
1	25 (40%)
2	8 (13%)
3	3 (5%)
4	3 (5%)
5	1 (2%)
6	1 (2%)
Imaging measures, median \pm IQR	
Baseline WMH Volume, % of TICV	0.43 \pm 0.78
24-hour Infarct Volume, mL	0.9 \pm 7.6
Times, median hours \pm IQR	
Symptom Discovery to MRI	3.2 \pm 5.1
Triage to MRI	1.2 \pm 1.6
Acute treatment	
	n (%)
Alteplase only	19 (26%)
Endovascular therapy only	8 (11%)
Alteplase plus endovascular	6 (8%)
Stroke etiology TOAST classification	
Large artery atherosclerosis	13 (18%)
Cardioembolism	17 (23%)
Small-vessel disease	14 (19%)
Other determined etiology	10 (14%)
Undetermined etiology	20 (27%)

mRS: modified Rankin Scale; NIHSS: NIH Stroke Scale; T-MoCA: telephone Montreal Cognitive Assessment; IQR: interquartile range; TICV: total intracranial volume.

Table 1. Demographic data.

Demographic data, $n=74$	
Age, mean \pm SD years	67 \pm 15
Women, n (%)	35 (47%)
Education >12 years, n (%)	69 (93%)
Ethnicity	
	n (%)
Caucasian	44 (59%)
Black	25 (34%)
Asian	3 (4%)
Hispanic	2 (3%)
Cerebrovascular risk factors	
	n (%)
Hypertension	54 (73%)
Hyperlipidemia	36 (49%)
Diabetes	18 (24%)
Prior stroke or TIA	11 (15%)
Atrial fibrillation	9 (12%)
Coronary artery disease	6 (8%)
Current or recent smoker	6 (8%)
Valvular heart disease	5 (7%)
Known cancer	5 (7%)
Prior intracerebral hemorrhage	4 (5%)
Cardiomyopathy	3 (4%)
Carotid artery disease	3 (4%)
Illicit drug use	1 (1%)

SD: standard deviation.

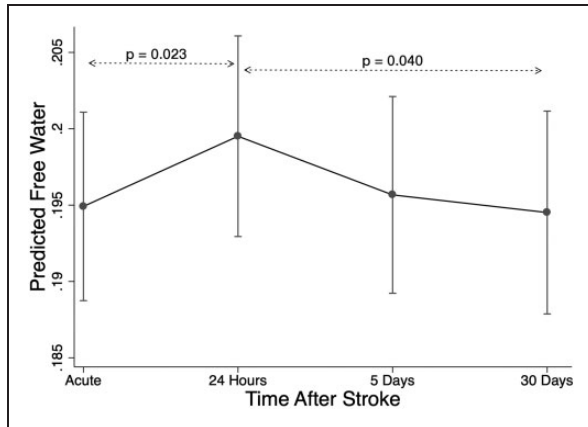


Figure 2. Change in global free water (FW) after stroke. Mixed-effects linear regression was used to estimate change in FW over timepoints, including covariates age, sex, NIHSS, infarct volume, and hospital site.

by 0.7% between 24 hours and 30 days (Beta = -6.86×10^{-6} , CI: -1.24×10^{-5} to 1.37×10^{-6} , $z = -2.45$, adjusted $p = 0.057$). However, in post-hoc analysis MD timepoint comparisons were not significantly different. Main effects included higher global MD in women (Beta = 2.1×10^{-5} , CI: 5.0×10^{-6} to 3.6×10^{-5} , $z = 2.5$, $p = 0.001$) and older patients (Beta = 1.7×10^{-6} , CI: 1.1×10^{-6} to 2.2×10^{-6} , $z = 6.0$, $p < 0.001$). Global FA, FA_{tissue}, and MD_{tissue} did not change over time. Given the temporal dynamics of increasing FW in the first 24 hours after stroke, we repeated the longitudinal analysis while excluding the 4 patients who reported initial symptoms more than 24 hours out. We found similar results, although notably 2 of these 4 did not have a 24-hour MRI. Furthermore, when we included time from symptom onset to MRI as an additional covariate, the results were unchanged. We also repeated the analysis excluding TIA patients and found similar results.

Since we identified main effects of higher global FW and MD in women while covarying for age, NIHSS, infarct volume, and hospital site, we further investigated baseline sex differences. Women had higher FW and MD at all timepoints but there was no sex by time interaction. There were no significant sex differences in clinical variables, but for women several non-significant differences were noted: mean age was older, mean baseline WMH volume was higher, mean NIHSS was higher, mean infarct volume was higher, and more women had cardioembolic stroke while fewer had large artery atherosclerotic strokes.

Acute global DTI metrics and cognitive performance

Associations between cognitive outcomes and white matter measures or covariates are presented in

Table 3 and Table 4. To understand the relationship between DTI metrics and cognitive performance, we first established multiple linear regression models incorporating relevant covariates: age, sex and variables with univariate associations with $p < 0.10$. White matter measures including WMH volume and each global DTI measure were then tested separately within this model. Higher global FW was associated with worse 30-day T-MoCA score ($n = 61$). Similar results were found for acute global MD, acute global MD_{tissue}, acute global FA, acute global FA_{tissue}, and WMH volume. Pre-stroke mRS was also associated with 30-day T-MoCA (See Table 4). Worse performance on the T-MoCA at 90 days ($n = 56$) was associated with acute global FW, acute global MD, acute global FA, acute global FA_{tissue}, and hospital site.

To further investigate the effect of hospital site on 90-day T-MoCA performance, we compared baseline demographics and clinical measures across hospital sites. Patients presenting to Washington Hospital Center who underwent 90-day T-MoCA were younger, more likely to be black, presented with more severe strokes, were more likely to receive acute recanalization therapy, and had larger 24-hour infarct volumes compared to patients presenting to Suburban Hospital. These patients also had lower functional status at 90-days as measured by the modified rankin score despite similar pre-stroke modified rankin score.

Given the novel finding of transiently increased global FW immediately after stroke onset described above, and the association between acute FW and cognitive performance, we also tested whether change in FW is associated with cognitive performance. To capture the effects of stroke-related global FW change, we imputed missing FW timepoints, which comprised 10% of the data, and calculated the area under the FW curve (AUC) over time for each subject. In multiply imputed, pooled regression analysis, acute global FW but not the stroke-related FW change, measured as AUC, was associated with 30-day T-MoCA and 90-day T-MoCA.

DTI changes within the acute ischemic lesion

For comparison, Figure 3 shows how these DTI measures changed over time within the infarct (which was excluded from the global analysis). FW in the infarct increased over time ($p < 0.001$) (Figure 3(a)) consistent with expected development of vasogenic edema. MD initially dropped and then increased (Figure 3(c)), consistent with typical patterns of restricted diffusion in an infarct. When the increasing FW signal was separated to measure only MD_{tissue}, the drop in diffusivity was larger and lasted longer (Figure 3(d)), again consistent with the known interplay between cytotoxic edema restricting extracellular diffusion while cell breakdown

Table 3. Univariate associations with follow-up telephone MoCA score.

	30-day T-MoCA (n = 61)		90-day T-MoCA (n = 56)	
	R ²	p	R ²	p
Age	0.05	0.080	0.0072	0.53
Female sex	0.01	0.46	0.0002	0.92
Education ≤12 years	0.06	0.060	0.0006	0.86
NIHSS initial	0.11	0.0080	0.10	0.016
Infarct volume	0.08	0.020	0.10	0.018
mRS pre-stroke	0.29	<0.0001	0.0052	0.60
Infarct location ^a	0.10	0.19	0.040	0.71
Hospital site	0.02	0.24	0.13	0.0068
Telephone vs in-person MoCA	0.002	0.73		
White matter measures				
WMH volume	0.14	0.0027	0.042	0.13
Global FW initial	0.13	0.0050	0.042	0.13
Global MD initial	0.14	0.0033	0.044	0.12
Global FA initial	0.20	0.0003	0.14	0.0038
Global MD _{tissue} initial	0.097	0.015	0.004	0.64
Global FA _{tissue} initial	0.19	0.0005	0.21	0.0003
Imputed FW AUC (t-statistic, p)	-1.36	0.18	-1.45	0.16

^aR² from Wald test for categorical regression.

T-MoCA: Telephone Montreal Cognitive Assessment; NIHSS: National Institutes of Health Stroke Scale; mRS: modified Rankin Score; FW: free water; MD: mean diffusivity; FA: fractional anisotropy; MD_{tissue}: MD in tissue compartment (FW corrected); FA_{tissue}: FA in tissue compartment; FW AUC: imputed area under the free water curve.

and accumulating vasogenic edema increases diffusivity and FW. FA decreased from the acute timepoint to each later timepoint (Figure 3(b)), but FA_{tissue} did not change over the 4 timepoints. For comparison we also evaluated the effect of these DTI measures from within the acute infarct on cognitive performance. DTI measures within the infarct were not associated with T-MoCA at 30 or 90 days.

Discussion

In this study, we found that global DTI measures, assessed at the time of an acute stroke, are associated with cognitive performance one month and three months later. We also found that global extracellular free water outside the infarcted tissue transiently increased in the brain over the first 24 hours after stroke onset, suggesting that focal ischemia has a diffuse effect on the brain, which we interpret as stroke-related inflammation. However, global DTI measures that are less effected by acute stroke, such as FA, were more associated with post-stroke cognitive performance than the stroke-related changes in global FW we detected between presentation and 24 hours. We conclude that in this population of relatively minor ischemic strokes and TIAs, baseline brain health is an important predictor of early post-stroke cognitive performance. However it remains to be determined if the transient changes in FW detected in this study have

an impact on long-term cognitive outcomes after stroke.

DTI measures microstructural white matter integrity and fluid shifts in the extracellular space, and so reflects both baseline brain health as well as acute stroke-related changes. DTI is sensitive to cognitive performance in healthy aging and across a range of neurologic diseases.⁴⁶ Large infarcts in strategic areas have a disproportionate effect on cognition,⁴⁷ but brain health is an expected determinant of 1) baseline cognitive performance 2) resilience to acute injury and 3) potential for recovery. The pre-stroke integrity of non-infarcted ipsilesional and the contra-lesional hemispheres may be an important determinant of how well stroke patients can compensate for acute injury. Other studies have demonstrated that leukoaraiosis and white matter DTI measures in remote regions are associated with poor cognitive performance^{4,7} and worse functional outcome^{48,49} in stroke patients.

In this study, global FA and FA_{tissue} remained relatively static after stroke and were most consistently associated with follow-up T-MoCA performance at 30 and 90 days. Global FA more likely reflects underlying brain health and is less affected by acute stroke than FW or MD. However, there were only small differences in the strengths of associations of global white matter measures and cognitive performance, due to collinearity, and a larger sample would be needed to

Table 4. Multiple regression associations with follow-up telephone MoCA scores.

Multitple regression for 30-day T-MoCA (n = 61)						
	Coefficient	95% CI	T	p	Change in Adjusted R ²	Change in AIC
mRS pre-stroke	-2.63	[-4.06 to -1.20]	-3.68	0.0005	0.16	-11.6
NIHSS initial	-0.24	[-0.53 to 0.050]	-1.66	0.10	0.02	-1.2
Education ≤12 years	-1.89	[-5.09 to 1.30]	-1.19	0.24	0.01	-2.8
Age	-0.18	[-0.07 to 0.040]	-0.64	0.52	-0.01	1.5
Sex	-0.32	[-1.87 to 1.24]	-0.41	0.69	-0.01	1.8
Infarct volume	0.019	[-0.11 to 0.15]	0.30	0.76	-0.01	1.9
Base Model	<i>Adjusted R² = 0.29</i>			<i>AIC = 310.16</i>		
White matter measures separately added to the bases model:						
	Coefficient	95% CI	T	p	New Adjusted R ²	New AIC
WMH volume	-0.98	[-1.88 to -0.08]	-2.19	0.033	0.34	306.8
Global FW initial	-37.52	[-63.01 to -12.03]	-2.95	0.0047	0.38	302.9
Global MD initial	-30481.78	[-49941.65 to -11021.91]	-3.14	0.0027	0.39	301.7
Global FA initial	46.39	[19.38 to 73.4]	3.45	0.0011	0.41	299.8
Global MD _{tissue} initial	-204199.20	[-351436.6 to -56961.8]	-2.78	0.0075	0.37	303.8
Global FA _{tissue} initial	58.40	[16.18 to 100.63]	2.77	0.0076	0.37	303.9
Imputed FW AUC	-1.35	[-5.11 to 2.4]	-0.75	0.46	n/a	n/a
Multitple regression for 90-day T-MoCA (n = 56)						
	Coefficient	95% CI	T	p	Change in adjusted R ²	Change in AIC
Hospital site	2.42	[0.33 to 4.50]	2.33	0.024	0.04	-3.7
Age	-0.048	[-0.11 to 0.011]	-1.64	0.11	0.03	-0.9
Sex	0.68	[-0.85 to 2.21]	0.89	0.38	-0.01	1.1
Infarct volume	-0.041	[-0.15 to 0.064]	-0.79	0.43	-0.01	1.3
NIHSS initial	-0.049	[-0.25 to 0.15]	-0.50	0.62	-0.02	1.8
Base model	<i>Adjusted R² = 0.14</i>			<i>AIC = 279.4</i>		
White matter measures separately added to the bases model:						
	Coefficient	95% CI	T	p	New Adjusted R ²	New AIC
WMH volume	-0.68	[-1.82 to 0.46]	-1.20	0.24	0.15	279.8
Global FW initial	-24.79	[-49.49 to -0.09]	-2.02	0.049	0.19	276.9
Global MD initial	-20330.49	[-39536.31 to -1124.67]	-2.13	0.039	0.20	276.4
Global FA initial	41.18	[14.30 to 68.05]	3.08	0.0034	0.27	271.5
Global MD _{tissue} initial	-73050.00	[-208025.60 to 61925.61]	-1.09	0.28	0.15	280.0
Global FA _{tissue} initial	63.11	[20.80 to 105.41]	3.00	0.0043	0.26	271.5
Imputed FW AUC	-1.69	[-5.53 to 2.15]	-0.94	0.36	n/a	n/a

T-MoCA: telephone Montreal Cognitive Assessment; T: T-statistic; AIC: Akaike Information Criterion; mRS: modified Rankin Scale; NIHSS: NIH Stroke Scale; WMH: white matter hyperintensity; FW: free water; MD: mean diffusivity; FA: fractional anisotropy; MD_{tissue}: MD corrected for free water; FA_{tissue}: FA corrected for free water; FW AUC: imputed area under the free water curve.

determine the best DTI metric to predict post-stroke cognitive impairment. But while acute global DTI measures were associated with follow-up T-MoCA scores, the global, dynamic change in FW, measured as AUC, was not associated with short-term cognitive

outcomes, which further supports the hypothesis that global brain health contributed more to cognitive outcome than transient changes in non-infarcted white matter in this sample of patients with relatively small infarcts.

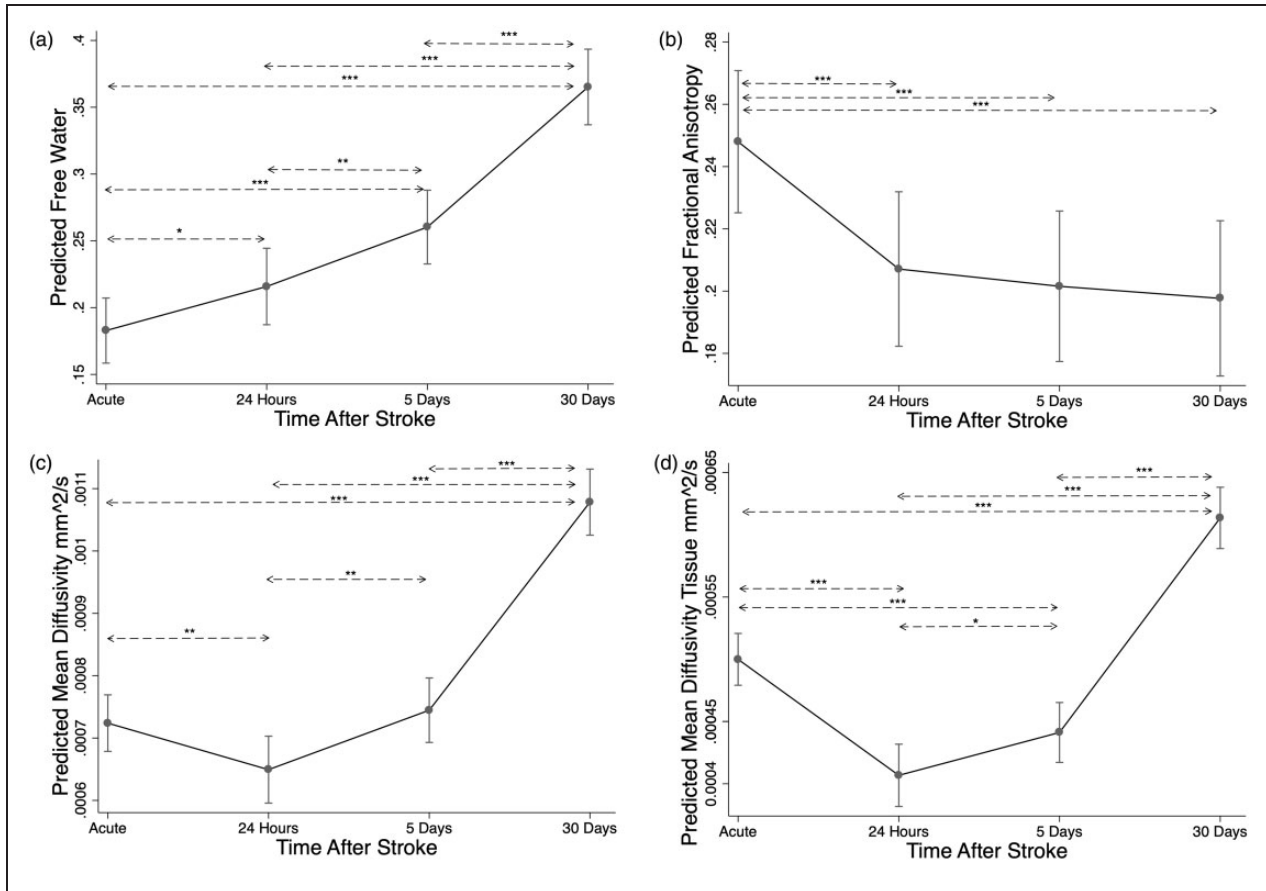


Figure 3. DTI changes within the infarct. For comparison, the changes in mean DTI metrics within the infarct after stroke were estimated using mixed-effects linear regression for: (a) free water (FW), (b) fractional anisotropy, (c) mean diffusivity, and (d) mean diffusivity in the tissue compartment corrected for FW (MD_{tissue}). *Adjusted $p < 0.05$. **Adjusted $p < 0.01$. ***Adjusted $p < 0.001$.

In this study, women had higher global FW and MD measures, and lower global FA measures relative to men across all timepoints, but these differences should be interpreted cautiously. Although baseline demographics were not significantly different, women were slightly older, had slightly worse baseline function, more cerebrovascular risk factors, larger stroke volumes, and greater baseline leukoaraiosis. Differences in stroke etiology were not significant, but more women had cardioembolic strokes and more men had large artery atherosclerotic strokes. DTI measures are sensitive to the multifactorial contributors to chronic cerebrovascular disease. Prior DTI studies of brain sex differences in better-matched cohorts have found that women have higher FA and lower radial diffusivity (possibly reflecting greater myelination) in central white matter structures.⁵⁰ A DTI study of sex differences in elderly and Alzheimer's participants found no FW differences in the elderly controls and reduced FW in women with Alzheimer's relative to men.⁵¹

Baseline clinical and imaging measures were more predictive of 30-day T-MoCA scores than 90-day scores (best R^2 0.41 vs. 0.27). Using an optimal cutoff of 18 on the T-MoCA for cognitive impairment³⁷ would label 40% as cognitively impaired at 30 days but only 22% with impairment at 90-days. Patients without 90-day follow-up had lower 30-day T-MoCA scores (15 vs 18) than those with follow-up. Longitudinal cognitive studies are often hampered by higher drop-out rates in lower performers.⁵² Cognitive assessments were mostly in-person for the 30-day visit, but via telephone for the 90-day assessment. We combined data using the telephone MoCA score, but this likely reduced our sensitivity for detecting cognitive impairment and reduced power to detect meaningful change.³⁷ For those who had both 30- and 90-day scores, the small relative score increase may reflect recovery from acute stroke, learning effects, or differences between telephone and in-person testing. We did not have pre-stroke cognitive measures to distinguish pre-stroke cognitive status from stroke-related

cognitive impairment. More detailed cognitive testing and longer follow-up would provide insight on whether DTI is useful in predicting more permanent cognitive changes after stroke or subsequent cognitive decline.

We also found that patients presenting to Medstar Washington Hospital Center had lower 90-day T-MoCA scores. Patients presenting to this urban D.C. comprehensive stroke center were younger with a trend for more cerebrovascular risk factors, and were more likely to be black. Among those that had 90-day cognitive testing, patients from Washington Hospital Center presented with more severe strokes, were more likely to undergo acute recanalization therapy, and had larger 24-hour infarct volumes. These patients also had higher mRS at 90 days despite similar baseline mRS relative to patients from Suburban hospital. The difference in hospital site 90-day cognitive outcomes may be partly driven by larger, more severe strokes with worse overall outcome, although there may also be additional environmental, demographic, recruitment, and retention biases that contribute.

DTI FW is a sensitive marker of chronic cerebrovascular injury and vascular cognitive impairment, but here we identify a relationship between global FW and cognitive performance in the acute stroke setting. Both FW and tissue components (corrected for FW) of the diffusion signal were associated with post-stroke cognitive performance, reinforcing the potential of FW as a useful imaging contrast separate from conventional metrics MD and FA. Furthermore, we demonstrated an acute, transient elevation in global FW in stroke patients between the measurement at presentation of the acute stroke and at 24 hours. The change in MD paralleled the change in FW, but to a lesser degree and did not survive correction for multiple comparisons. This MD change was likely driven by the change in the FW compartment, since no change was seen in MD_{tissue} .

There are several possible explanations for this transient elevation in FW after stroke. One hypothesis is that an acute change in global FW reflects diffuse vasogenic edema as part of a global inflammatory response to acute stroke. Increased inflammatory cytokines and cellular infiltration may lead to blood-brain barrier disruption and vasogenic edema globally. Previous studies have demonstrated dynamic changes remote from the acute ischemic infarct including elevated markers of systemic inflammation,^{53,54} remote microglial activation within 2 weeks of stroke using ^{11}C -PK11195 positron emission tomography (PET),⁵⁵ and increased blood-brain barrier permeability using dynamic contrast-weighted MRI.^{14,48,56} We saw that on average FW returned to near initial values by 30 days, but the magnitude and duration of this response may be variable, and further longitudinal studies should evaluate

whether the degree of FW change relates to neuroinflammation or predicts long term consequences of stroke.

We used a DTI sequence with a single high B-value, or single shell, to quantify global FW, which limits the interpretation of our FW results. Multi-shell methods require longer scan times but provide a more accurate measurement of the fast-diffusing FW compartment.^{25,57} Local tissue perfusion also contributes 1–3% to the fast component of the diffusion signal in healthy subjects.⁵⁷ However, in a 2-compartment diffusion model, the FW compartment includes this perfusion signal, which may overestimate the FW fraction, particularly when using single-shell DTI data. So, increased local perfusion may also contribute to the change in global FW after stroke. With more non-zero, low B-values, the perfusion signal can be modeled as a separate compartment using intravoxel incoherent motion (IVIM) diffusion imaging and a 3-compartment model,⁵⁷ which would allow differentiation of the local perfusion and measured FW.

We also demonstrate a steady increase in FW within the infarcted tissue after ischemic stroke. This FW increase is expected as vasogenic edema develops in and around the infarcted tissue, similar to what is seen on FLAIR imaging between 3 and 6 hours after stroke onset.⁵⁸ Vasogenic edema is associated with stroke outcome even in non-malignant infarcts.^{59,60} However, the FW signal continues to rise even after the period when vasogenic edema is expected to wane. This is likely due to loss of tissue architecture, encephalomalacia and cavitation, such that CSF comprises a larger fraction of the region of interest. Therefore, dynamic FW changes should be interpreted in the setting of other FW-corrected DTI metrics. In contrast to FW, MD (aka ADC) initially decreases as cytotoxic edema restricts the diffusivity of water in the extracellular space, then normalizes and increases due to both cell lysis and development of vasogenic edema. Pseudo-normalization of MD, when the MD returns to normal values despite underlying tissue injury, has also been attributed to glial infiltration in studies using complementary kurtosis DTI.⁶¹ We found the initial decrease in MD_{tissue} to be more pronounced and prolonged than conventional MD when the effect of the FW compartment was removed. MD_{tissue} has previously been shown to predict lesion cavitation in subcortical infarcts when measured in the first week after stroke. Future studies should assess whether MD_{tissue} can distinguish true diffusion weighted imaging reversal (e.g. due to successful recanalization) from pseudo-normalization and whether it better predicts final infarct volume.

While our study is unique in acquiring serial DTI on acute stroke patients, there are several limitations

related to the heterogeneity of our stroke population. For one, the timing of acute imaging relative to last-known well time and symptom discovery was not uniform. This may have decreased our statistical power to detect acute global changes in additional DTI metrics, although we found similar results when excluding patients with symptoms starting more than 24 hours before acute MRI. A study of tPA treated patients only may provide a more homogenous population to better characterize the time-dependence of acute FW changes. Including TIA patients in this study may have also reduced the effect size of acute FW changes we detected. However, we predict that transient ischemia would also elicit a stroke-related inflammatory response. Similarly, excluding these patients did not appreciably alter the results. Treatment and revascularization were variable as well, and reperfusion may lead to a different pattern in the dynamic DTI changes after stroke.

With regard to generalizability, we caution that our study is biased toward minor stroke patients with low NIHSS and small infarct volumes. These patients were more likely to be recruited in the acute stroke setting and more capable of participating in cognitive testing at 30 and 90-days. We predict that in a population of more severe strokes, acute infarct characteristics such as infarct volume and stroke location will contribute more to post-stroke cognitive performance. Future studies should evaluate global FW as a marker of cerebral edema in large hemispheric infarcts, since novel investigational treatment trials are targeting edema to improve stroke outcomes.^{62,63} Finally, rapid DTI acquisition in the acute stroke setting is not feasible in many stroke centers, which limits the generalizability of these results.

In conclusion, DTI with FW correction enables the study of brain health at the time of an acute ischemic stroke and its relation to post-stroke cognitive performance. FW measurement provides a new metric for assessing global changes in the brain during and after acute stroke. In this study of relatively minor strokes, global DTI metrics provided a measure of brain health that was associated with early post-stroke cognitive performance. We detected a transient elevation in global FW in the first 24-hours after acute stroke that we interpret as stroke-related inflammation. While this change was not related to post-stroke cognitive performance, future studies should investigate how these acute DTI changes impact longitudinal white matter degeneration and long-term cognitive outcomes.

Funding

The author(s) disclosed receipt of the following financial support for the research, authorship, and/or publication of this article: This study was fully funded by the Intramural

Research Program of the National Institute of Neurological Disorders and Stroke (NINDS), National Institutes of Health, Bethesda, MD, USA.

Acknowledgements

The authors thank Ying Kuen Cheung, Ph.D. and Paul Juneau M.S. for statistical expertise and Larry Latour, Ph. D. for study oversight and intellectual input. The authors thank the stroke programs at MedStar Washington Hospital and Suburban Hospital. This work utilized the computational resources of the NIH HPC Biowulf cluster: hpc.nih.gov.

Declaration of conflicting interests


The author(s) declared the following potential conflicts of interest with respect to the research, authorship, and/or publication of this article: Dr. Wright receives royalties from UpToDate.com for topics on vascular dementia. Dr. Kern and Dr. Leigh have no disclosures.

Authors' contributions

KCK contributed to study design, data collection, analysis, and manuscript preparation. CBW contributed to study design, analysis, and manuscript preparation. RL contributed to study design, data collection, analysis, and manuscript preparation.

ORCID iDs

Kyle C Kern  <https://orcid.org/0000-0002-2703-7669>

Richard Leigh  <https://orcid.org/0000-0002-8285-1815>

Supplemental material

Supplemental material for this article is available online.

References

1. Gottesman RF and Hillis AE. Predictors and assessment of cognitive dysfunction resulting from ischaemic stroke. *Lancet Neurol* 2010; 9: 895–905.
2. Desmond DW, Moroney JT, Sano M, et al. Incidence of dementia after ischemic stroke. *Stroke* 2002; 33: 2254–2262.
3. Ivan CS, Seshadri S, Beiser A, et al. Dementia after stroke: the Framingham study. *Stroke* 2004; 35: 1264–1268.
4. Chaudhari TS, Verma R, Garg RK, et al. Clinico-radiological predictors of vascular cognitive impairment (VCI) in patients with stroke: a prospective observational study. *J Neurol Sci* 2014; 340: 150–158.
5. Levine DA, Galecki AT, Langa KM, et al. Trajectory of cognitive decline after incident stroke. *JAMA* 2015; 314: 41–51.
6. Kliper E, Ben Assayag E, Tarrasch R, et al. Cognitive state following stroke: the predominant role of preexisting white matter lesions. *PLoS One* 2014; 9: e105461.
7. McMurtray AM, Liao A, Haider J, et al. Cognitive performance after lacunar stroke correlates with leukoaraiosis severity. *Cerebrovasc Dis* 2007; 24: 271–276.

8. Kumral E, Güllüoğlu H, Alakbarova N, et al. Cognitive decline in patients with leukoaraiosis within 5 years after initial stroke. *J Stroke Cerebrovasc Dis* 2015; 24: 2338–2347.
9. Reijmer YD, Fotiadis P, Piantoni G, et al. Small vessel disease and cognitive impairment: the relevance of central network connections. *Hum Brain Mapp* 2016; 37: 2446–2454.
10. Schaapsmeeders P, Tuladhar AM, Arntz RM, et al. Remote lower white matter integrity increases the risk of Long-Term cognitive impairment after ischemic stroke in young adults. *Stroke* 2016; 47: 2517–2525.
11. Du J, Wang Y, Zhi N, et al. Structural brain network measures are superior to vascular burden scores in predicting early cognitive impairment in post stroke patients with small vessel disease. *Neuroimage Clin* 2019; 22: 101712.
12. Park J-Y, Kim Y-H, Chang WH, et al. Significance of longitudinal changes in the default-mode network for cognitive recovery after stroke. *Eur J Neurosci* 2014; 40: 2715–2722.
13. Aben HP, Biessels GJ, Weaver NA, et al. Extent to which network hubs are affected by ischemic stroke predicts cognitive recovery. *Stroke* 2019; 50: 2768–2774.
14. Villringer K, Sanz Cuesta BE, Ostwaldt AC, et al. DCE-MRI blood-brain barrier assessment in acute ischemic stroke. *Neurology* 2017; 88: 433–440.
15. Shi K, Tian D-C, Li Z-G, et al. Global brain inflammation in stroke. *Lancet Neurol* 2019; 18: 1058–1066.
16. Nilupul Perera M, Ma HK, Arakawa S, et al. Inflammation following stroke. *J Clin Neurosci* 2006; 13: 1–8.
17. Vila N, Castillo J, Dávalos A, et al. Proinflammatory cytokines and early neurological worsening in ischemic stroke. *Stroke* 2000; 31: 2325–2329.
18. Kliper E, Bashat DB, Bornstein NM, et al. Cognitive decline after stroke: relation to inflammatory biomarkers and hippocampal volume. *Stroke* 2013; 44: 1433–1435.
19. Pierpaoli C, Jezzard P, Basser PJ, et al. Diffusion tensor MR imaging of the human brain. *Radiology* 1996; 201: 637–648.
20. Le Bihan D, Mangin JF, Poupon C, et al. Diffusion tensor imaging: concepts and applications. *J Magn Reson Imaging* 2001; 13: 534–546.
21. O’Sullivan M, Summers PE, Jones DK, et al. Normal-appearing white matter in ischemic leukoaraiosis: a diffusion tensor MRI study. *Neurology* 2001; 57: 2307–2310.
22. Pasi M, van Uden IW, Tuladhar AM, et al. White matter microstructural damage on diffusion tensor imaging in cerebral small vessel disease: Clinical consequences. *Stroke* 2016; 47: 1679–1684.
23. Pierpaoli C and Jones DK. Removing CSF contamination in brain DT-MRIs by using a two-compartment tensor model. *Proc Intl Soc Mag Reson Med* 2004; 11: 12–15.
24. Pasternak O, Sochen N, Gur Y, et al. Free water elimination and mapping from diffusion MRI. *Magn Reson Med* 2009; 62: 717–730.
25. Golub M, Neto Henriques R and Gouveia Nunes R. Free-water DTI estimates from single b-value data might seem plausible but must be interpreted with care. *Magn Reson Med* 2021; 85: 2537–2551.
26. Maillard P, Mitchell GF, Himali JJ, et al. Aortic stiffness, increased white matter free water, and altered microstructural integrity: a continuum of injury. *Stroke* 2017; 48: 1567–1573.
27. Zhang R, Huang P, Jiaerken Y, et al. Venous disruption affects white matter integrity through increased interstitial fluid in cerebral small vessel disease. *J Cereb Blood Flow Metab* 2021; 41: 157–165.
28. Duering M, Finsterwalder S, Baykara E, et al. Free water determines diffusion alterations and clinical status in cerebral small vessel disease. *Alzheimer’s Dementia* 2018; 14: 764–774.
29. Maillard P, Fletcher E, Singh B, et al. Cerebral white matter free water: a sensitive biomarker of cognition and function. *Neurology* 2019; 92: e2221–e2231.
30. Altendahl M, Maillard P, Harvey D, et al. An IL-18-centered inflammatory network as a biomarker for cerebral white matter injury. *PLoS One* 2020; 15: e0227835.
31. Hoy AR, Ly M, Carlsson CM, et al. Microstructural white matter alterations in preclinical Alzheimer’s disease detected using free water elimination diffusion tensor imaging. *PLoS One* 2017; 12: e0173982.
32. Bergamino M, Pasternak O, Farmer M, et al. Applying a free-water correction to diffusion imaging data uncovers stress-related neural pathology in depression. *Neuroimage Clin* 2016; 10: 336–342.
33. Lesh TA, Maddock RJ, Howell A, et al. Extracellular free water and glutathione in first-episode psychosis—a multimodal investigation of an inflammatory model for psychosis. *Mol Psychiatry* 2021; 26: 761–771.
34. Dacosta-Aguayo R, Grana M, Fernandez-Andujar M, et al. Structural integrity of the contralesional hemisphere predicts cognitive impairment in ischemic stroke at three months. *PLoS One* 2014; 9: e86119.
35. Zamboni G, Griffanti L, Jenkinson M, et al. White matter imaging correlates of early cognitive impairment detected by the Montreal cognitive assessment after transient ischemic attack and minor stroke. *Stroke* 2017; 48: 1539–1547.
36. Nasreddine ZS, Phillips NA, Bedirian V, et al. The Montreal cognitive assessment, MoCA: a brief screening tool for mild cognitive impairment. *J Am Geriatr Soc* 2005; 53: 695–699.
37. Pendlebury ST, Welch SJ, Cuthbertson FC, et al. Telephone assessment of cognition after transient ischemic attack and stroke: modified telephone interview of cognitive status and telephone Montreal cognitive assessment versus face-to-face Montreal cognitive assessment and neuropsychological battery. *Stroke* 2013; 44: 227–229.
38. Smith SM, Jenkinson M, Woolrich MW, et al. Advances in functional and structural MR image analysis and implementation as FSL. *Neuroimage* 2004; 23 Suppl 1: S208–S219.
39. Garyfallidis E, Brett M, Amirbekian B, et al. Dipy, a library for the analysis of diffusion MRI data. *Front Neuroinform* 2014; 8: 8.

40. Andersson JLR and Sotiropoulos SN. An integrated approach to correction for off-resonance effects and subject movement in diffusion MR imaging. *Neuroimage* 2016; 125: 1063–1078.
41. Golub M. Implementation of an algorithm for estimating free-water fraction in diffusion-weighted magnetic resonance imaging. *Instituto Superior Tecnico* 2018; 1–73.
42. Griffanti L, Zamboni G, Khan A, et al. BIANCA (brain intensity AbNormality classification algorithm): a new tool for automated segmentation of white matter hyperintensities. *Neuroimage* 2016; 141: 191–205.
43. Smith SM, Johansen-Berg H, Jenkinson M, et al. Acquisition and voxelwise analysis of multi-subject diffusion data with tract-based spatial statistics. *Nat Protoc* 2007; 2: 499–503.
44. Schmidt P, Gaser C, Arsic M, et al. An automated tool for detection of FLAIR-hyperintense white-matter lesions in multiple sclerosis. *Neuroimage* 2012; 59: 3774–3783.
45. StataCorp. *Stata statistical software: release 13*. 13 ed. College Station, TX: StataCorp LP, 2013.
46. Sullivan EV and Pfefferbaum A. Diffusion tensor imaging and aging. *Neurosci Biobehav Rev* 2006; 30: 749–761.
47. Zhao L, Biesbroek JM, Shi L, et al. Strategic infarct location for post-stroke cognitive impairment: a multivariate lesion-symptom mapping study. *J Cereb Blood Flow Metab* 2018; 38: 1299–1311.
48. Rost NS, Cougo P, Lorenzano S, et al. Diffuse microvascular dysfunction and loss of white matter integrity predict poor outcomes in patients with acute ischemic stroke. *J Cereb Blood Flow Metab* 2018; 38: 75–86.
49. Sagnier S, Catheline G, Dilharreguy B, et al. Normal-appearing white matter integrity is a predictor of outcome after ischemic stroke. *Stroke* 2020; 51: 449–456. DOI: doi:10.1161/STROKEAHA.119.026886.
50. Shin YW, Kim DJ, Ha TH, et al. Sex differences in the human corpus callosum: diffusion tensor imaging study. *Neuroreport* 2005; 16: 795–798.
51. Bergamino M, Keeling EG, Baxter LC, et al. Sex differences in Alzheimer's disease revealed by free-water diffusion tensor imaging and Voxel-Based morphometry. *J Alzheimers Dis* 2022; 85: 395–414.
52. Schaie KW, Labouvie GV and Barrett TJ. Selective attrition effects in a fourteen-year study of adult intelligence. *J Gerontol* 1973; 28: 328–334.
53. Rothenburg LS, Herrmann N, Swardfager W, et al. The relationship between inflammatory markers and post stroke cognitive impairment. *J Geriatr Psychiatry Neurol* 2010; 23: 199–205.
54. Narasimhalu K, Lee J, Leong YL, et al. Inflammatory markers and their association with post stroke cognitive decline. *Int J Stroke* 2015; 10: 513–518.
55. Thiel A, Radlinska BA, Paquette C, et al. The temporal dynamics of poststroke neuroinflammation: a longitudinal diffusion tensor imaging-guided PET study with ¹¹C-PK11195 in acute subcortical stroke. *J Nucl Med* 2010; 51: 1404–1412.
56. Arba F, Leigh R, Inzitari D, et al. Blood-brain barrier leakage increases with small vessel disease in acute ischemic stroke. *Neurology* 2017; 89: 2143–2150.
57. Rydhog AS, Szczepankiewicz F, Wirestam R, et al. Separating blood and water: Perfusion and free water elimination from diffusion MRI in the human brain. *Neuroimage* 2017; 156: 423–434.
58. Thomalla G, Cheng B, Ebinger M, et al. DWI-FLAIR mismatch for the identification of patients with acute ischaemic stroke within 4.5 h of symptom onset (PRE-FLAIR): a multicentre observational study. *Lancet Neurol* 2011; 10: 978–986.
59. Battay TW, Karki M, Singhal AB, et al. Brain edema predicts outcome after nonlacunar ischemic stroke. *Stroke* 2014; 45: 3643–3648.
60. Kim Y, Luby M, Burkett N-S, et al. Fluid-attenuated inversion recovery hyperintense ischemic stroke predicts less favorable 90-day outcome after intravenous thrombolysis. *Cerebrovasc Dis* 2021; 50: 738–738.
61. Weber RA, Hui ES, Jensen JH, et al. Diffusional kurtosis and diffusion tensor imaging reveal different time-sensitive stroke-induced microstructural changes. *Stroke* 2015; 46: 545–550.
62. King ZA, Sheth KN, Kimberly WT, et al. Profile of intravenous glyburide for the prevention of cerebral edema following large hemispheric infarction: evidence to date. *Drug Des Devel Ther* 2018; 12: 2539–2552.
63. Pergakis M, Badjatia N, Chaturvedi S, et al. BIIB093 (IV glibenclamide): an investigational compound for the prevention and treatment of severe cerebral edema. *Expert Opin Investig Drugs* 2019; 28: 1031–1040.